frontiers | Frontiers in Materials

TYPE Original Research
PUBLISHED 06 April 2023
DOI 10.3389/fmats.2023.1144752

OPEN ACCESS

EDITED BY
Yuanfei Wang,
Qingdao Stomatological Hospital, China

REVIEWED BY
Tong Wu,
Qingdao University, China
Dawei Li,
Jiangnan University, China

*CORRESPONDENCE
Shih-Feng Chou,
schou@uttyler.edu

SPECIALTY SECTION
This article was submitted to Biomaterials and Bio-Inspired Materials, a section of the journal Frontiers in Materials

RECEIVED 15 January 2023
ACCEPTED 28 March 2023
PUBLISHED 06 April 2023

CITATION
Gizaw M, Bani Mustafa D and Chou S-F (2023), Fabrication of drug-eluting polycaprolactone and chitosan blend microfibers for topical drug delivery applications.
Front. Mater. 10:1144752.
doi: 10.3389/fmats.2023.1144752

Fabrication of drug-eluting polycaprolactone and chitosan blend microfibers for topical drug delivery applications

Mulugeta Gizaw, Diala Bani Mustafa and Shih-Feng Chou*

Department of Mechanical Engineering, College of Engineering, The University of Texas at Tyler, Tyler, TX, United States

Chronic and non-healing wounds show delayed and incomplete healing process, which expose the patients to a high risk of infection. These types of wounds require frequent change of dressing, which is a burden on the patients. In addition, ideal dressing needs to meet the requirements in minimizing microbial infiltration and growth while balancing moisture and exchanging oxygen with outside environment. To overcome the challenge in frequent change of dressing and meet the design requirements, current researches have focused on the development of electrospun fibers with incorporation of small molecule drugs for sustained release purpose. In this study, electrospinning was performed to fabricate blend fibers consisting of 15 wt% of polycaprolactone (PCL) and 4 wt% of chitosan (CS) at various blend ratios with the incorporation of a model small molecule drug, acetylsalicylic acid (ASA). Results showed that fibers became more hydrophilic when increasing CS concentration from 0% to 60% in PCL/CS blank fibers. Increasing CS concentration decreased fiber diameter resulting in the decrease of fiber mechanical properties. Furthermore, the addition of 10% w/w ASA also made the fibers more hydrophilic and further decreased the fiber diameter. There were no linear relationships between CS concentrations and fiber mechanical properties in the drug-loaded samples, which indicated some level of drug-polymer interactions. Fiber mechanical properties and drug release rates were two major aspects indicative of strong and/or weak drug-polymer interactions. *In vitro* drug release in PBS buffer solution showed a burst profile of ASA (30%) up to 2 h followed by a zero-order release rate up to 2 days.

KEYWORDS

electrospun fibers, polycaprolactone, chitosan, drug release, mechanical properties

1 Introduction

Chronic and/or non-healing wounds take considerably a longer than usual of time to heal. Clinical care of chronic and/or non-healing wounds requires frequent change of dressing materials, which is a painful process for the patients. It also generates social and economical burden for patients with chronic and/or non-healing wounds. Hence, there is an urgent need in the development of advanced biomaterials as an alternative dressing material to replace traditional wound healing cream/gels. The ideal dressing materials are considered as a drug delivery system that needs to carry a high amount of drug (> 10%) while achieving controlled-release behaviors to prevent overdosing. A wide variety of antimicrobial agents have been incorporated in fiber-based materials for sustained release purpose in wound

dressing (Gizaw et al., 2018). However, most these small molecule drugs were hydrophobic agents, where their gradual release rates from drug carriers were due to the poor solubility in media. Hydrophilic agents represent a major challenge in achieving sustained release behaviors due to their abilities to alter the overall hydrophilicity of the carrier and their high solubility in release media (Chou et al., 2015).

Electrospinning is a simple, robust, and cost-effective method to produce drug-containing fibers with diameters ranging from tens of nanometers to several micrometers (Chou et al., 2015; Emerine and Chou, 2022). The result is a layer of non-woven fiber mesh that exhibits the texture of typical textiles with a porous structure allowing drainage of the wound exudates and permeation of atmospheric oxygen to the wound (Saghazadeh et al., 2018). In addition to these advantages, electrospinning accepts various types of small molecule drugs as well as the inclusion of other nano-scaled drug delivery systems (e.g., nanoparticles and micellles) to serve as a composite dressing material suitable for multi-stage controlled release purpose in wound healing (Schneider et al., 2009). The working principle behind electrospinning involves the application of a high electric field between the fiber collecting plate and the tip of a needle, which is attached to a syringe that contains the polymer solution. The surface tension of the droplet forming at the tip of the needle (i.e., Taylor cone) is overcome by the electrostatic repulsion force that causes a stream of continuous fiber depositing on the collector. The solvents present in the polymer solution evaporate rapidly due to a high surface area to volume ratio of the fiber as it travels to the collecting plate forming a fiber mesh (Chou and Woodrow, 2017).

Several studies have investigated the use of natural and synthetic polymers in electrospun fibers as wound dressing materials for sustained delivery of drugs (Wang and Windbergs, 2017; Gizaw et al., 2018). Among all natural materials, chitosan (CS) showed excellent intrinsic properties against fungi and bacteria growth making it suitable for wound dressing materials (Dai et al., 2011; Cooper et al., 2013; Sapkota and Chou, 2020). CS is the *N*-deacetylated product of chitin, and it is soluble in water and under acidic conditions due to the protonation of amino groups (Aranaz et al., 2021). Results suggested that CS fiber structure and morphology as well as overall hydrophobicity determined the drug release rate. The presence of rigid D-glucosamine makes CS solutions very viscous and difficult to electrospin alone. As a result, it is usually electrospun in conjunction with other synthetic polymers. Polycaprolactone (PCL) is one of the most studied synthetic biomaterials in electrospun fibers due to its biocompatibility, slow biodegradability ($t_{1/2}$ > 18 months (Peña et al., 2006)), and easy forming of fibers. PCL at room temperature is a semi-crystalline aliphatic polyester with T_g around −60°C and T_m around 55°C–60°C resulting in a tensile strength of 28 MPa and an elastic modulus of 217 MPa (Wachirahuttapong et al., 2016). PCL has limited applications before blending other polymers due to its high hydrophobicity, slow degradation, and lack of functional groups (Roozbahani et al., 2013; Liverani et al., 2018). Therefore, the combination of PCL and CS in electrospun fibers may be a potential drug carrier for wound dressing materials.

Our previous work showed that the ability to achieve sustained release of a hydrophilic small molecule drug from blends of hydrophobic polymers was mainly due to drug-polymer interactions investigated by mechanical testing (Chou and Woodrow, 2017). In addition, we observed tunable drug release rates through drug dissolution and diffusion in blend fibers of ethyl cellulose and polyethylene oxide (Hawkins et al., 2022). In this study, we extend our investigation on drug release behaviors and mechanical properties from blend PCL and CS fibers with the incorporation of a hydrophilic model drug, acetylsalicylic acid (ASA). The hypothesis is that composition of CS and loading of ASA play an important role in determining drug release rate and mechanical properties of the PCL/CS fibers. We investigated the fiber morphologies and average fiber diameters of PCL/CS fibers at various blend compositions for potential use as drug carriers in dressing materials. Average elastic moduli and tensile strength showed effects of CS compositions and incorporation of ASA without clear evidence of plasticizing effects. Fibers wettability studies showed an improved wetting behavior with increasing of CS composition and loading of hydrophilic ASA in the PCL/CS blend fibers, where fast release of ASA from PCL/CS fibers indicated drug dissolution.

2 Materials and methods

2.1 Materials

Polycaprolactone (PCL) (M_W ~ 80 kDa) was purchased from Huaian Ruanke Co., Ltd. (China). Chitosan (CS) (degree of deacetylation: 90%) was supplied by Xi'an ZhongYun Biotechnology Co., Ltd. (China). USP grade acetylsalicylic acid (ASA), an experimental model drug, was purchased from Thermo Fisher Scientific Inc. (Waltham, MA, United States). Hexafluoro-2-propanol (HFIP), 99% purity, was purchased from Richest Group Ltd. (China). Glacial acetic acid (AA), 99.7% minimal ACS, was supplied by BDH® Avantor (Radnor, PA, United States). Biotechnology grade phosphate-buffered saline (PBS) solution, pH 7.3–7.5, containing 137 mM sodium chloride, 2.7 mM potassium chloride, and 10 mM phosphate buffer, was purchase from Avantor (Radnor, PA, United States). Deionized (DI) water was obtained from Chemistry Department at the University of Texas at Tyler.

2.2 Preparation of PCL/CS solutions

15 wt% (wt/vol) PCL solution was prepared by dissolving PCL beads in pure HFIP solvent according to our previous study (Chou and Woodrow, 2017). 4 wt% CS solutions of were prepared by dissolving CS powder in 90% AA solution, which was obtained by volumetric mixing of AA and DI-water. Both PCL and CS solutions were set on a rotisserie mixer at room temperature overnight to create homogeneous polymer solutions.

After reaching homogeneous PCL and CS solutions in separate vials, blend PCL/CS solutions of 100/0, 80/20, 60/40, and 40/60 were created by volumetric mixing of the corresponding polymer solutions. ASA-loaded polymer solutions were prepared by adding 10% of ASA in PCL/CS solutions (w/w = drug/total solids) and stirred for 2 h.

To study the effects of PCL weight percentage on the overall mass of the polymer fibers, 17.75 wt% and 22.33 wt% of PCL solutions were prepared separately using the same procedure as described above. The 17.75 wt% and 22.33 wt% PCL solutions were mixed with 4 wt% CS solution at 80/20 and 60/40 volumetric fractions, respectively. These modifications allowed the total polymer weight percentage to be same as 15 wt% pure PCL solution.

2.3 Electrospinning of PCL/CS nanofibers

2 mL of PCL/CS solution was loaded in a 3 mL BD Luer-Lok™ syringe and secured on a New Era syringe pump (Farmingdale, NY, United States). A 21-gauge stainless steel dispensing needle was attached to the syringe and was connected to the positive voltage source from Gamma High Voltage (Ormond Beach, FL, United States). The negative end was connected to a stationary-grounded collector plate covered with a layer of wax paper. During electrospinning, the flow-rate was set to 20 μL/min, the applied voltage was 15 kV, and the distance between the tip of the needle and the collector plate was 10 cm. Once the electrospinning was done, the fiber mats were stored in a vacuum desiccator to remove excess solvents.

2.4 Fiber morphologies and average fiber diameters

Scanning electron microscopy (SEM) was used to investigate the fiber morphologies and average fiber diameters of electrospun PCL/CS fibers. In brief, circular punches of the fiber meshes were sputter coated with Au/Pd for 30 s using a SPI sputter-coater (West Chester, PA, United States) at 80–100 mTorr. SEM micrographs were acquired from a filament typed SEM system at LeTourneau University (Longview, TX, United States) at 15 kV, using a spot size 3, and a working distance of 15.0 cm. Images taken from SEM were analyzed by ImageJ software, National Institutes of Health (Bethesda, MD, United States), for average fiber diameters (n = 30).

2.5 Fiber mat uniformity and porosity

To study the effects of PCL and CS concentrations and PCL/CS blends on the distributions of fiber depositions, thickness of electrospun PCL/CS fiber mats at various locations were was measured using a digital thickness gauge (resolution = 1 μm) on a squared grid system.

Fiber mat porosities were determined by the apparent density method. In brief, thickness and weight of 7/16" fiber disc punches were measured to determine the apparent density (He et al., 2005). The bulk densities of the blend polymers were then calculated using the theoretical densities (i.e., PCL = 1.145 g/cm^3 and CS = 0.25 g/cm^3). The fiber mat porosities were determined by the ratio of apparent to bulk densities.

2.6 Mechanical testing

Mechanical testing was performed on an Instron® 3,342 universal material tester (Norwood, MA, United States) in accordance with ASTM standard D882-18 under 24°C ± 1°C and 45% ± 5% RH (ASTM D882-18, 2018). A dog-bone shaped fiber specimen with 22 mm nominal length and 5 mm nominal width were cut out using a stainless steel die (ODC Tooling and Molds, Waterloo ON, Canada) in accordance with ASTM 1708-18 (ASTM D1708-18, 2018). The thickness of each sample was measured using a digital thickness gauge (resolution = 1 μm). The test was performed with a constant strain rate of 0.01/s. Stress and strain was calculation from the raw load and displacement data for each sample. A total of 3 specimens were used for each fiber composition (n = 3).

2.7 Water contact angle measurements

To measure the water contact angle, a 4-μL DI-water droplet was dispensed on a dry fiber sample at room temperature. The water contact angle was determined by the angle between the surface and the contact tangent using ImageJ software, National Institutes of Health (Bethesda, MD, United States). To observe the dynamic change of the water contact angle, images at various time points, up to 60 s, were taken for measurements. Results were average of three independent measurements (n = 3).

2.8 *In-vitro* drug release

7/16″diameter circular disks were taken from electrospun fibers mats using a metal die. The thickness of each sample was measured using a digital thickness gauge (resolution = 1 μm) and their respective mass was measured using an analytical balance. The samples were placed into glass vials containing 10 mL of PBS buffer solution pre-heated to 37°C for sink drug release. For the reminder of the experiment, the PBS (pH 7.3–7.5) solution containing fiber samples were kept in a rotary incubator with 120 rpm at 37°C. At pre-determined time points, up to 48 h, a 200-μL liquid sample containing unknown concentration of ASA was taken from each glass vial and placed in HPLC vials followed by refilling with 200-μL fresh PBS to compensate for the lost of volume.

The collected liquid samples were then analyzed using a Waters e2695 high-performance liquid chromatography (HPLC) (Milford, MA, United States) equipped with a C18 column. The HPLC mobile phase consisted of 50% HPLC graded DI-water with 0.045% trifluoroacetic acid buffer and 50% acetonitrile. The parameters included 30°C column, 1 mL/min flow rate, 5 min run time, 10 μL sample injection volume and UV/vis detection at 225 nm.

The ASA standard curve was generated by dissolving 4 mg of ASA in 20 mL of PBS solution followed by serial dilutions to solution concentrations of 100, 50, 10, and 0.1 μg/mL. All drug release data were collected from triplicates and used to report mean and standard deviation of the sample (n = 3).

2.9 Statistical analysis

Results were expressed as average ± standard deviation (SD). Statistical studies of the averages were performed using GraphPad Prism (San Diego, CA, United States) on one-way analysis of variance (ANOVA). Significance was accepted with $p < 0.05$.

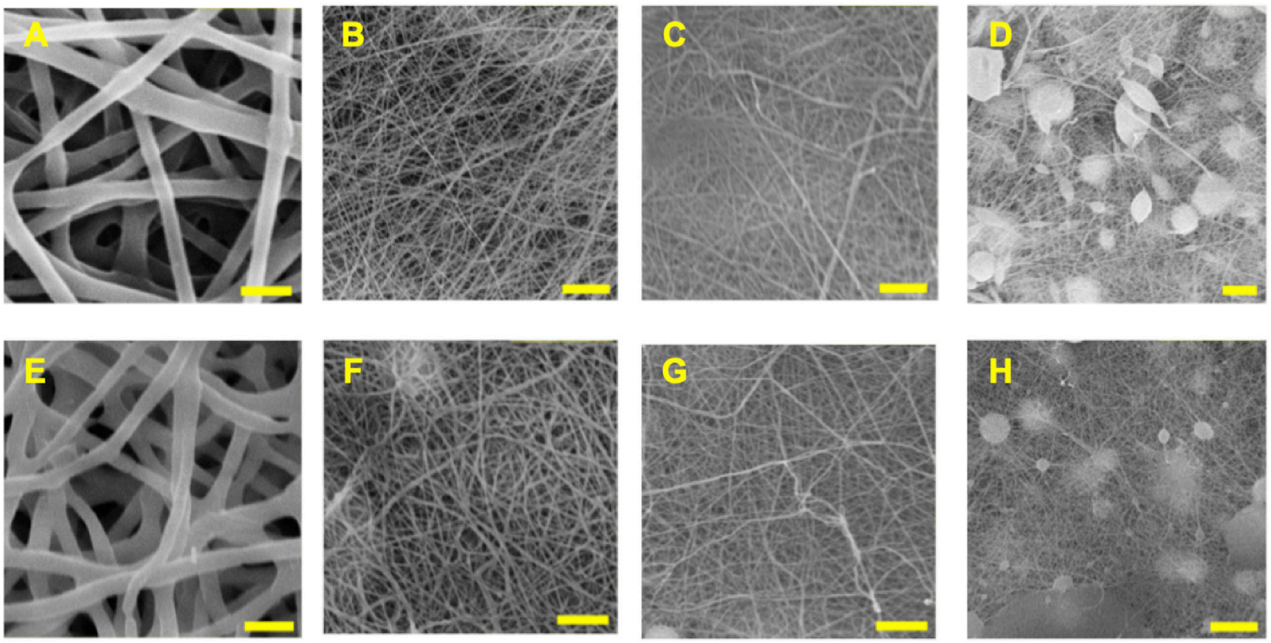

FIGURE 1
SEM images of electrospun PCL/CS blend fibers at various compositions. The top row shows blank PCL/CS fibers of **(A)** 100/0, **(B)** 80/20, **(C)** 60/40, and **(D)** 40/60 compositions. The bottom row shows the ASA-loaded PCL/CS fibers of **(E)** 100/0, **(F)** 80/20, **(G)** 60/40, and **(H)** 40/60 compositions. Scale bar = 5 μm.

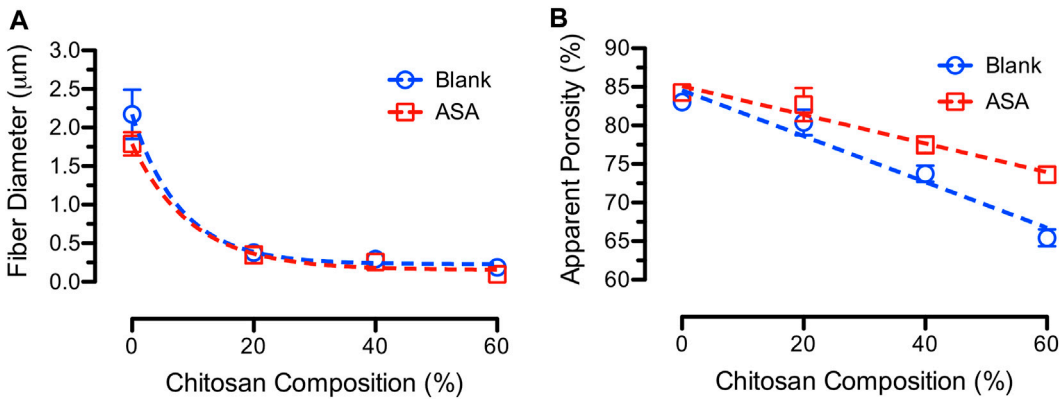

FIGURE 2
(A) Average fiber diameter and **(B)** average fiber mat porosity for blank and ASA-loaded PCL/CS fibers at various CS compositions.

3 Results and discussion

3.1 Fiber morphology

Fiber morphologies from electrospun blank and ASA-loaded PCL/CS fibers at various blend ratios were investigated using SEM. As shown in Figure 1, smooth and defect-free fibers were obtained from blend PCL/CS fibers with blend ratios of 100/0, 80/20, and 60/40. Formations of beads and large wet spots were observed in 40/60 PCL/CS fibers. ASA-loaded PCL/CS fibers showed no morphological changes as well as no drug crystallization as compared to the blank fibers. No fiber formations were observed for the 20/80 and 0/100 PCL/CS blend fibers. Chitosan has a rigid molecular structure that inhibits the electrospinnability of the PCL/CS blend polymer solutions (Qasim et al., 2018).

3.2 Average fiber diameters and fiber mat porosities

The average fiber diameters for electrospun blank and ASA-loaded PCL/CS fibers at various blend ratios are shown in Figure 2A.

The average fiber diameters for blank and ASA-loaded 100/0 PCL/CS fibers were 2.17 ± 0.32 μm and 1.79 ± 0.15 μm, respectively. Increasing CS composition in the blend PCL/CS fibers significantly decreased the average fiber diameters to 0.19 ± 0.02 μm and 0.10 ± 0.03 μm for blank and ASA-loaded PCL/CS fibers, respectively. The decrease in average fiber diameter was due to a decrease of the overall polymer concentration when mixing 15 wt% of PCL with 4 wt% of CS. Interestingly, the average fiber diameters of ASA-loaded PCL/CS fibers were smaller than those of the blank fibers. Since the electrospinning parameters were kept the same for all fiber formulations, the smaller average fiber diameter of the ASA-loaded fibers suggested an improved electrospinnability. Studies had shown that polymer solution properties and electrospinning parameters affected the average fiber diameters (Tan et al., 2005). For instance, fibers electrospun with 10 wt% PCL (120–300 kDa) exhibited fiber diameters between 0.44–1.04 μm (Baker et al., 2016). Others electrospun PCL/CS fibers using 1 wt% CS and 10 wt% PCL in HFIP, where the fiber diameter was 200 nm for 1 wt% chitosan and 730 nm for 10 wt% PCL (Yang et al., 2009).

Average fiber mat porosity is described by apparent porosity that represents the empty space between the neighboring fibers. A highly porous dressing is desired for cell attachment and growth, adsorption of the wound exudates, and permeation of atmospheric oxygen to the wound (Aghdam et al., 2012). Porous fiber mats also encourage cell proliferation attributed to cell infiltration and exchange of oxygen and nutrients (Poornima and Korrapati, 2017). It also provides mechanical support of newly formed tissue by interlocking the fibers with the surrounding tissue (Loh and Choong, 2013). However, the mechanical properties of the fibers will become poor if the fiber mats are too porous. Hence, there is a balance between the fiber mat porosity and the desired mechanical properties. Figure 2B shows the average apparent porosities for blank and ASA-loaded PCL/CS blend fiber mats at various CS compositions. The average apparent porosities decreased from 83.0% ± 0.6% to 65.4% ± 1.1% and from 84.3% ± 0.8% to 73.6% ± 1.1% for blank and ASA-loaded PCL/CS fibers, respectively. Literature recommends electrospun scaffolds used for tissue engineering application to exhibited an average fiber mat porosity that is higher than 80% (Ferreira et al., 2014). Others reported the porosity in the range of 70%–90% for electrospun fiber mats (Croisier et al., 2012). Fiber mat porosity varies with the types of fibers being electrospun. For instance, PCL/PLA blends in ratio of 4/1 resulted in a fiber mat porosity of up to 77.2%, and the fiber mat porosity for pure PCL was 72.9% (Yao et al., 2017).

3.3 Fiber mat uniformity

Electrospun fibers produced from syringe/nozzle assembly with a stationary collector plate generate circular-shaped fiber mats due to the "whipping" process of the polymer jets. To investigate the effect of solution properties on fiber mat uniformity, a grid system was used to measure the thickness of the fiber mat at fixed locations. Figure 3 shows the topological profiles of blank and ASA-loaded PCL fibers electrospun from 15 wt% and 20 wt% PCL solutions. Results suggested that incorporation of ASA in PCL solutions produced a fiber mat with a larger deposition area due to the improved "whipping" ability of the fibers. This observation was in accordance with the decrease in average fiber diameter due to fiber stretching associated with a stronger "whipping" behavior. In addition, increasing polymer solution concentration showed a minimal effect in the fiber deposition area. Our results demonstrated the dependence of fiber mat uniformity with the inclusion of small molecule drugs.

3.4 Mechanical properties of PCL/CS fibers

Literature suggested that types of polymers and solvents, electrospinning parameters, fiber diameter and morphology, and fiber mat porosity influenced the mechanical properties of electrospun fibers (Tan et al., 2005). To understand the mechanical responses of the blank and ASA-loaded PCL/CS blend fibers, dog-bone specimens of fibers were stretched with a strain rate of 0.01/s. Representative stress-strain curves for the blank and ASA-loaded PCL/CS fibers at various blend ratios are shown in Figure 4. All samples exhibited an initial linear viscoelastic region followed by a yield region of plastic deformation until reaching maximum stress for fracture. According to the stress-strain curves, blending CS in PCL fibers significantly reduced the elongation of the fibers. Incorporation of ASA in PCL/CS fibers decreased the elongation to failure as well as tensile stress in some of the PCL/CS compositions. However, it was unclear if ASA served the role of a plasticizer in PCL/CS blend fibers, which could indicate drug-polymer interactions.

The mechanical strength of PCL/CS fiber mats may be feasible for skin wound care since the average elastic modulus of human skin is 83.3 ± 34.9 MPa in addition to the average tensile strength of 21.6 ± 8.4 MPa and elongation of 54.0% ± 17.0% (Hendriks et al., 2006; Pailler-Mattei et al., 2008; Kim et al., 2012). Figure 5 shows the average elastic moduli and tensile strength of blank and ASA-loaded PCL/CS fibers at various CS compositions. The average elastic moduli ranged from 5.7 ± 0.7 MPa to 21.8 ± 1.1 MPa and from 3.2 ± 0.9 MPa to 14.3 ± 1.7 MPa for blank and ASA-loaded PCL/CS fibers, respectively. Furthermore, studies showed that tensile strength of 7 wt% PCL fibers was 3.13 MPa with elongation up to 96.3% (Wang et al., 2017). Furthermore, the average tensile stress ranged from 0.49 ± 0.24 MPa to 2.16 ± 0.18 MPa and from 0.33 ± 0.08 MPa to 1.77 ± 0.17 MPa for blank and ASA-loaded PCL/CS fibers, respectively. Studies showed that increasing the fiber diameter increased the tensile strength and elastic modulus of PCL fibers (Baji et al., 2010). Others reported a higher modulus (307 ± 6 MPa) and tensile strength (58 ± 4) of electrospun fibers as compared to those fabricated by compression molding (Wong et al., 2008). Another factor that could affect the elastic modulus of the electrospun fibers is the alignment of the fibers. For example, poly (vinylidene fluoride) (PVDF) received elastic moduli of 225 MPa, 27 MPa, and 23 MPa for the 0°, 45°, and 90° in fiber alignment, respectively (Maciel et al., 2018). In addition, fibers made from 1 wt% CS and 10 wt% PCL at various blend ratios showed a decrease in mechanical properties when increasing CS concentration in the blend fibers (Yang et al., 2009).

3.5 Surface wettability of electrospun PCL/CS fibers

Our previous studies showed that surface wettability of electrospun drug-eluting fibers determined the *in-vitro* drug

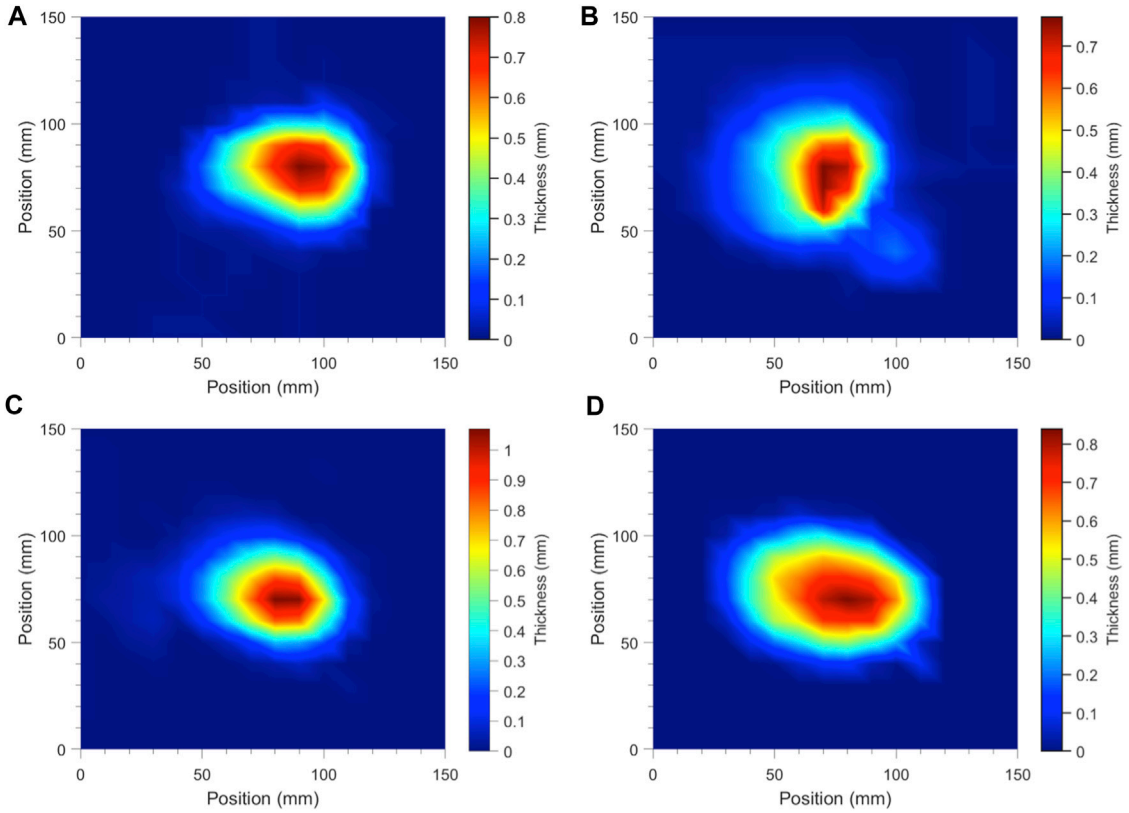

FIGURE 3
Temperature plots of topological PCL fiber mat profiles electrospun from needle/syringe and stationary collector setup to represent fiber mat uniformity, showing **(A)** 15% blank PCL, **(B)** ASA-loaded 15% PCL, **(C)** 20% blank PCL, and **(D)** ASA-loaded 20% PCL.

release rates. Specifically, blending water-soluble CS with hydrophobic PCL is expected to change the surface wettability of the PCL/CS fibers (Wang et al., 2017). The average water contact angles as a function of time for blank and ASA-loaded PCL/CS fibers are shown in Figure 6. As seen from the figure, the average water contact angles for both 100/0 and 80/20 blank PCL/CS fibers stayed above 90° during the time of observation. For 60/40 and 40/60 blank PCL/CS fibers, the initial average water contact angles were above 90° followed by a decrease to 0° within 80 s. The results suggested that increasing CS composition in the PCL/CS fibers increased the overall wettability of the fiber mats. In contrast, incorporation of ASA in the PCL/CS fibers promoted the surface wettability of the fiber mats for the 80/20 PCL/CS fibers. Average water contact angles for the rest of the ASA-loaded samples containing CS showed a decrease with time. The results suggest that both the incorporation of a hydrophilic drug (i.e., ASA) and the increase of CS composition in PCL/CS blend fibers promoted the overall wettability of the PCL/CS fiber mats. Our results were in accordance with a study using PLAA/CS fibers, where the water contact angle decreased as the concentration of CS increased in the blend fibers (Cui et al., 2012). Others demonstrated that surface wettability of the electrospun fibers played an important role in cell attachment (Kim et al., 2012; Wang et al., 2017; de Cassan et al., 2018). This property enables the opportunity in cell culture, cell delivery, and/or promoting cell growth locally, which is essential in wound healing.

3.6 *In vitro* ASA release from PCL/CS fibers

Figure 7 shows the standard curve of ASA and *in vitro* ASA release profiles from various compositions of electrospun PCL/CS fibers. The 100/0 PCL/CS fibers exhibited a slow release behavior over 48 h, while the rest of the PCL/CS fibers displayed a burst release characteristic. Specifically, the 100/0 PCL/CS fibers released 25% of ASA at the 2-h time point followed by a zero-order release rate up to 48 h. In addition, the 80/20 and PCL/CS samples achieved a complete release of ASA after 4 h, while the 60/40 and 40/60 PCL/CS fibers achieved complete releases of ASA at 1-h time point. Our findings demonstrated the effects of surface wettability of the electrospun PCL/CS fibers due to the presence of CS that promoted the fast release of a hydrophilic small molecule drug.

Studies showed that hydrophobic PCL slowed down the release of a hydrophilic drug in aqueous PBS while water-soluble CS promoted the fast release (Park et al., 2006; Kim et al., 2012). Others showed that PCL fibers were relatively stable in PBS solution after 14 days, while CS fibers showed significant level of degradation after 1 day resulting in rapid release of drug molecules (Yang et al., 2009). Although the presence of CS is highly desirable in wound dressing due to its antimicrobial properties (Ahmed and Ikram, 2016), the incorporation of hydrophilic drugs and the CS composition in wound dressing enhance drug release rates that result in early depletion of the therapeutic agents.

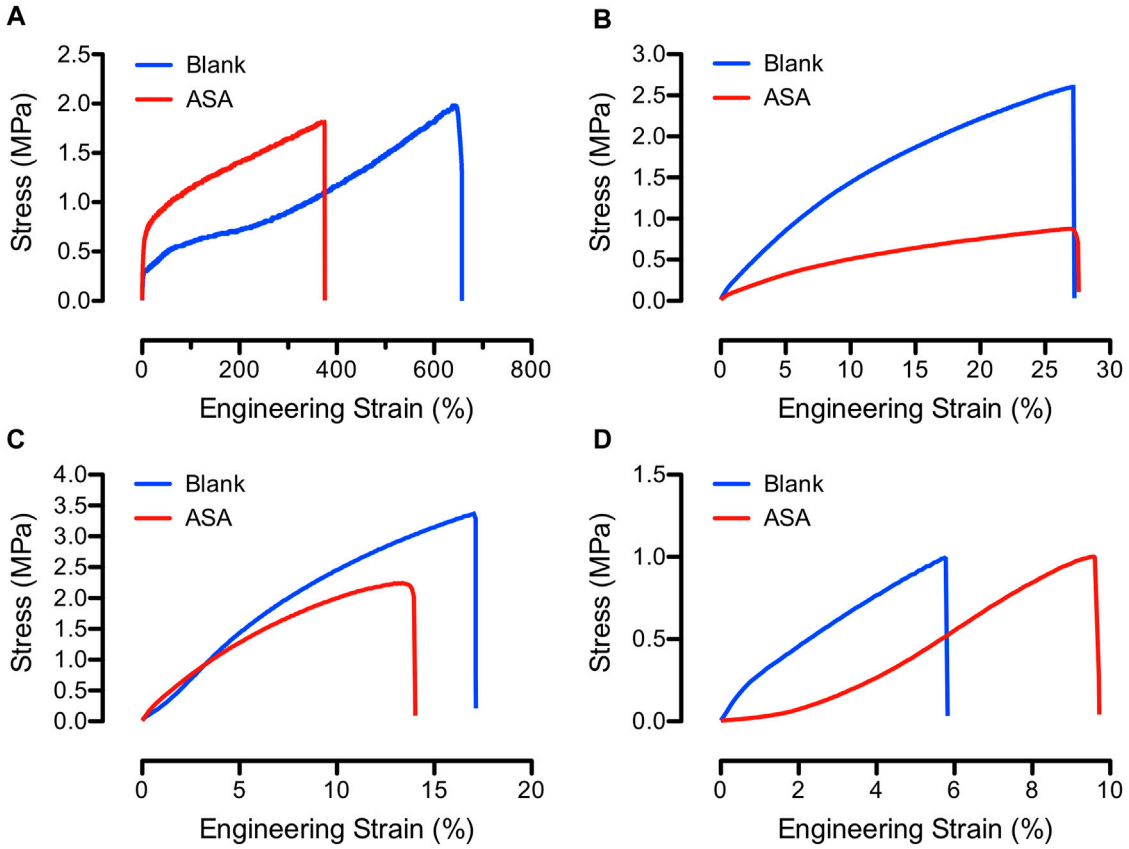

FIGURE 4
Engineering stress-strain curves of representative blank (blue) and ASA-loaded (red) PCL/CS blend fibers, showing **(A)** 100/0, **(B)** 80/20, **(C)** 60/40, and **(D)** 40/60 PCL/CS compositions.

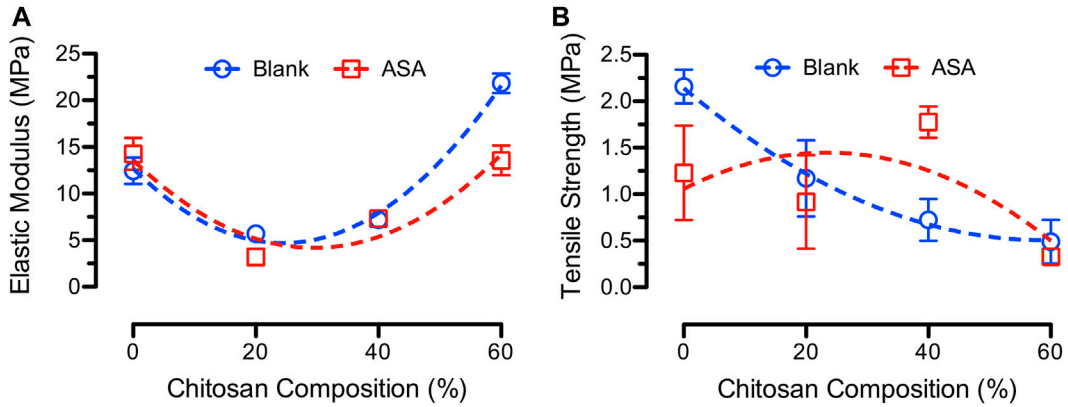

FIGURE 5
(A) Average elastic moduli and **(B)** average tensile strength of blank (blue) and ASA-loaded (red) PCL/CS blend fibers at various CS compositions.

3.7 Effects of PCL concentrations on PCL/CS fibers

As previously observed in the fiber morphology and average fiber diameter, increasing CS composition in the blend PCL/CS fibers promoted the formation of beads and a smaller average fiber diameter. To compensate for the decrease of overall polymer concentration in the blend PCL/CS solutions, in this section, the wt% of PCL were increased prior to mixing with 4 wt% chitosan to keep the overall concentrations of blend PCL/CS solution at 15 wt%.

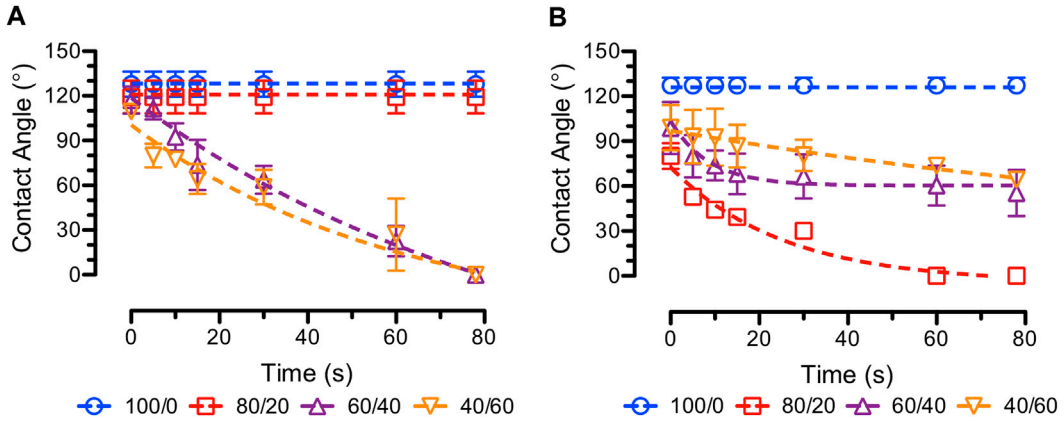

FIGURE 6
Average water contact angles over time (e.g., dynamic contact angles) of **(A)** blank **(B)** ASA-loaded PCL/CS fiber samples at various PCL/CS compositions.

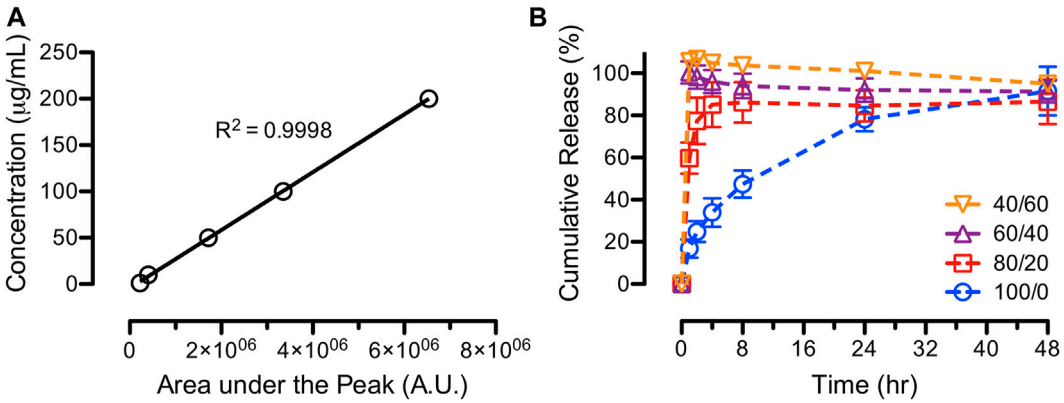

FIGURE 7
In-vitro release studies of ASA from PCL/CS blend fibers, showing **(A)** standard curve of known concentrations and **(B)** cumulative releases of ASA over 48 h for various PCL/CS blend fibers.

For example, in 80/20 and 60/40 PCL/CS compositions, PCL concentrations were increased to 17.75 wt% and 22.33 wt% to achieve the overall polymer concentration of 15 wt%. In addition, the 40/60 PCL/CS composition required 31.50 wt% of PCL in HFIP for mixing with 4 wt% of CS, where the PCL solution was too viscose to work in blend polymer solution. Therefore, the 40/60 PCL/CS fibers were excluded from the studies on the effects of PCL concentrations in PCL/CS fibers.

3.7.1 Fiber morphology and average fiber diameters

Figure 8 shows the SEM images and the average fiber diameters of PCL/CS blend fibers after adjusting the PCL concentrations. According to the images, PCL/CS fibers exhibited uniform surface morphology with a defect free structure. Studies demonstrated that fiber morphologies changed drastically based on the polymer concentration in electrospinning. For example, increasing PCL concentration from 14 to 26 wt% increased zero shear viscosity of the solution from 4.4 to 81 Pa s (Ferreira et al., 2014). At high PCL concentration, electrospun fibers typically received a larger diameter with a fused web structure between the adjacent fibers.

The average fibers diameter decreased from 2.17 ± 0.32 μm, 0.80 ± 0.09 μm, to 0.60 ± 0.15 μm for 100/0, 80/20, and 60/40 blank PCL/CS fibers, respectively. The average fiber diameter of the ASA-loaded PCL/CS fibers also decreased from 1.79 ± 0.15 μm, 0.76 ± 0.12 μm, to 0.52 ± 0.05 μm for 100/0, 80/20, and 60/40 compositions, respectively. While the average fiber diameters decreased with increasing CS compositions, the average fiber diameters for the 80/20 and 60/40 PCL/CS blend modified fibers were higher than those with a fixed PCL concentration (i.e., 15 wt%). In addition, a similar trend of smaller average fiber diameters was observed for ASA-loaded fibers when comparing with the blank fibers. Studies showed that increasing PCL concentration in the

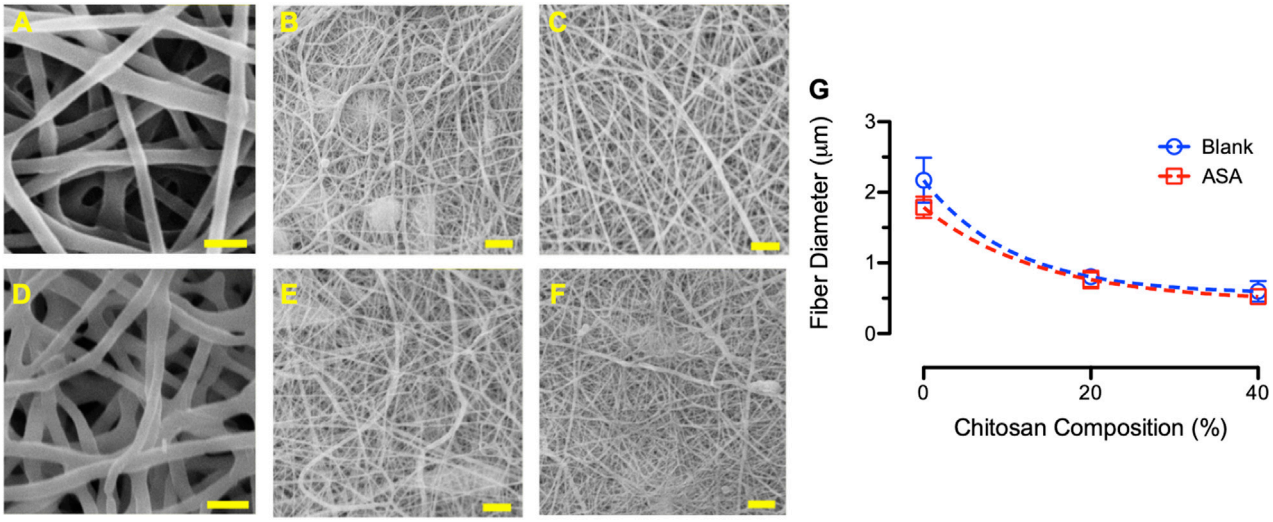

FIGURE 8
SEM images of electrospun PCL/CS fibers, showing **(A)** blank 100/0 composition using 15% PCL, **(B)** blank 80/20 composition using 17.75% PCL, **(C)** blank 60/40 composition using 22.33% PCL, **(D)** ASA-loaded 100/0 composition using 15% PCL, **(E)** ASA-loaded 80/20 composition using 17.75%, and **(F)** ASA-loaded 60/40 composition using 22.33% PCL. Scale bar = 5 μm. **(G)** Average fiber diameter of blank (blue) and ASA-loaded (red) blend PCL/CS fibers after modifying the PCL concentrations at various CS compositions.

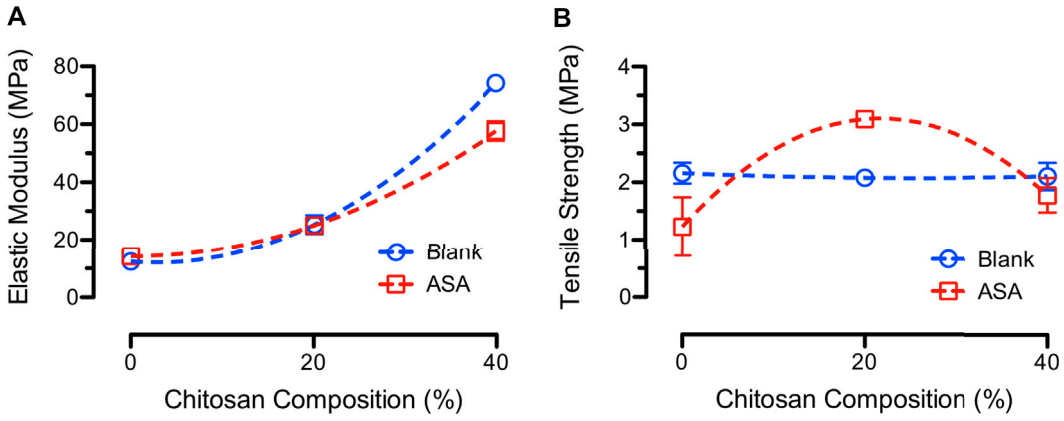

FIGURE 9
(A) Average elastic moduli and **(B)** average tensile strength of blank (blue) and ASA-loaded (red) PCL/CS blend fibers after modifying the PCL concentrations at various CS compositions.

polymer solution resulted in the formation of thicker fibers, while higher CS concentration resulted in thinner fibers (Yao et al., 2014). Others showed that increasing PCL concentration from 16 wt% to 22 wt% resulted in a better fiber morphology with an increase in fiber diameter (e.g., from 190 nm to 384 nm) (Li et al., 2018).

3.7.2 Mechanical properties

Figure 9 shows the average elastic moduli and tensile strength of various PCL/CS blend fibers after modifying the PCL concentrations. Results showed that the average elastic moduli of the fiber mats increased with increasing CS compositions in the blend PCL/CS fibers. For example, the average elastic moduli of blank 80/20 and 60/40 PCL/CS fibers increased to 25.4 ± 3.2 MPa and 74.2 ± 0.5 MPa as compared to those of the PCL/CS fibers electrospun from 15 wt% PCL. The same trend of increasing in elastic moduli was found in the ASA-loaded fibers. Average tensile strength for the 17.75 and 22.33 wt% blank fibers were 2.08 ± 0.05 MPa and 2.10 ± 0.25 MPa, respectively. The average tensile strength for the 17.75 and 22.33 wt% ASA-loaded PCL/CS fibers were 3.09 ± 0.14 MPa and 1.77 ± 0.30 MPa, respectively.

Effects of PCL concentrations on mechanical properties of nanofibers were reported by several studies. For example, studies showed that 75/25 PCL/CS blend fibers exhibited a higher modulus than the 50/50 PCL/CS fibers due to an improved inter-connectivity

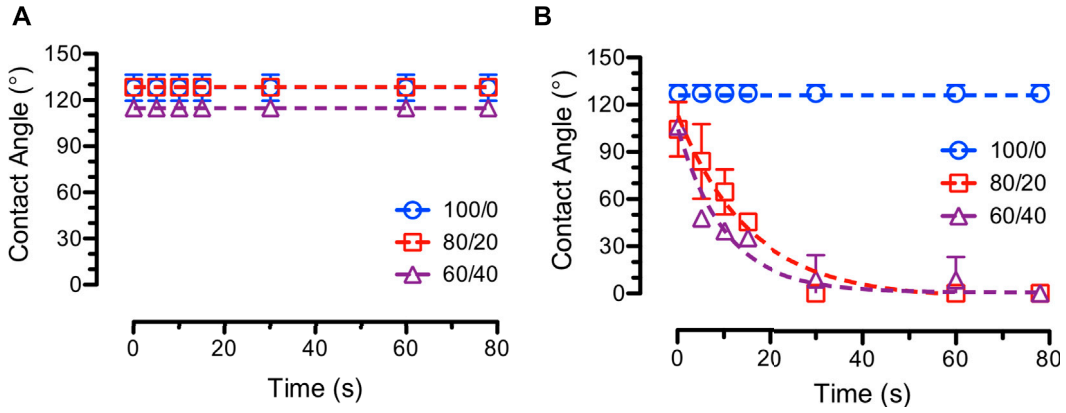

FIGURE 10
Average water contact angles over time (e.g., dynamic contact angles) of **(A)** blank **(B)** ASA-loaded PCL/CS fiber samples on the effects of modifying PCL concentrations (e.g., 100/0 = 15%/4% PCL/CS, 80/20 = 17.75%/4% PCL/CS, and 60/40 = 22.33%/4% PCL/CS).

of the fibers (Sarasam and Madihally, 2005). Others showed a change in Young's modulus and elongation at break for electrospun scaffold of PCL/CS with different CS compositions (3%–23%) (Trinca et al., 2017). The findings suggested the dependence of mechanical properties of PCL/CS fibers on both polymer concentration and composition of the blend fibers. The main factor that altered the mechanical properties of drug-loaded fibers was the interactions between the drug and polymer (Chou and Woodrow, 2017). The mechanical properties of scaffolds designed for topical wound dressing should be at least greater than that of the skin itself (tensile strength of 2–16 MPa and elastic modulus of 6–40 MPa). A good dressing material is expected to have good mechanical properties, biocompatibility, and antimicrobial properties (Trinca et al., 2017).

3.7.3 Fiber wettability

The effects of modifying PCL concentrations on fiber wettability of PCL/CS blend fibers were studied using water contact angle experiments over time. Since PCL is a hydrophobic polymer, it is expected that increasing PCL concentrations in various blends of PCL/CS fibers will increase the average water contact angles. Figure 10 shows the results from the various blends of PCL/CS fibers on the effects of modifying PCL concentrations. According to the results, all blank fibers exhibited a hydrophobic surface. Interestingly, incorporation of a hydrophilic small molecule drug (i.e., ASA) promoted the surface wettability of the blend PCL/CS fibers. This finding suggested that surface drugs on electrospun fibers were capable of alter their surface wettability. In general, polymer matrix (e.g., PCL concentrations in the blend PCL/CS fibers) and surface drugs determined the surface wettability of the electrospun fiber mats.

3.7.4 *In-vitro* ASA release

In-vitro ASA release assays were performed on various blends of PCL/CS fibers electrospun from modified PCL concentrations. The release curves, as shown in Figure 11, displayed the same fast release characteristics as observed from the original 80/20 and 60/40 PCL/CS fibers (Section 3.6) despite using more PCL in making the blend PCL/CS fibers. This finding was in accordance with the surface

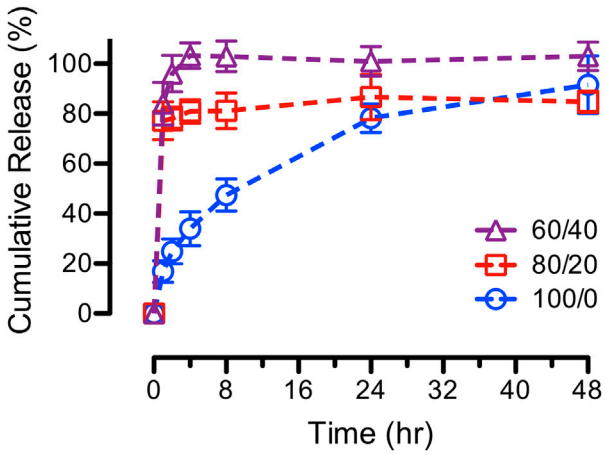

FIGURE 11
In-vitro cumulative release curves of ASA from various blends of PCL/CS fibers on the effects of modifying PCL concentrations (e.g., 100/0 = 15%/4% PCL/CS, 80/20 = 17.75%/4% PCL/CS, and 60/40 = 22.33%/4% PCL/CS).

wettability study in the previous section that the ASA-loaded PCL/CS blend fibers exhibited a hydrophilic surface, which promoted drug diffusion and dissolution. Studies showed that a less burst release followed by a steady release profile was mainly due to the incorporation of hydrophobic PCL to water-soluble chitosan (Surucu and Turkoglu Sasmazel, 2016). PCL is usually added to nanofibers composition to slow down the drug release rate, and hence, achieving a controlled release. For example, PCL was incorporated with collagen fibers to slow down the burst release of insulin (Kanungo et al., 2013).

The effect of PCL concentrations on alendronate release was reported using samples containing 2 and 4 wt% PCL (Bose et al., 2018). Results showed a slower burst release of drug molecules (34% and 26%, respectively) as compared to samples containing no PCL, which demonstrated a burst release up to 75% within 24-h period.

Others implemented PCL nanofibers as a layer of coating to slow down drug release rate (Xue et al., 2009; Tarafder et al., 2013; Tarafder and Bose, 2014). Most drug delivery systems exhibit initial burst release due to the interaction between drug molecules and releasing medium, especially for hydrophilic small molecules (e.g., ASA).

4 Conclusion

In this study, various compositions of PCL/CS fibers intended for uses of topical dressings were successfully developed using electrospinning. The use of a hydrophilic model drug was compatible at 10% loading. The fibers showed good morphology and mechanical properties. *In vitro* drug release showed a burst release of at 2-h time point followed by gradual release. To compensate the loss of solution properties in PCL/CS solutions when increasing CS compositions, an additional study was carried out to investigate PCL concentrations in the blend solutions for electrospinning. Results demonstrated an increase in average fibers diameter, fiber surface wettability, and fiber mechanical properties of the modified PCL/CS blend fibers while still maintaining the burst release characteristics. Our findings suggest a strong dependence on polymer fiber compositions and physicochemical properties of the small molecule drugs on the mechanical properties and *in-vitro* release rate of the blend fibers.

Data availability statement

The original contributions presented in the study are included in the article/supplementary material, further inquiries can be directed to the corresponding author.

Author contributions

MG and SFC contributed to conception and design of the study. DBM organized the database. MG and SFC performed the statistical analysis. MG wrote the first draft of the manuscript. DBM and SFC wrote sections of the manuscript. All authors contributed to manuscript revision, read, and approved the submitted version.

Acknowledgments

The authors thank the Ben and Maytee Fisch College of Pharmacy at the University of Texas at Tyler for providing access to a HPLC.

Conflict of interest

The authors declare that the research was conducted in the absence of any commercial or financial relationships that could be construed as a potential conflict of interest.

Publisher's note

All claims expressed in this article are solely those of the authors and do not necessarily represent those of their affiliated organizations, or those of the publisher, the editors and the reviewers. Any product that may be evaluated in this article, or claim that may be made by its manufacturer, is not guaranteed or endorsed by the publisher.

References

Aghdam, R. M., Najarian, S., Shakhesi, S., Khanlari, S., Shaabani, K., and Sharifi, S. (2012). Investigating the effect of PGA on physical and mechanical properties of electrospun PCL/PGA blend nanofibers. *J. Appl. Polym. Sci.* 124, 123–131. doi:10.1002/app.35071

Ahmed, S., and Ikram, S. (2016). Chitosan based scaffolds and their applications in wound healing. *Achiev. Life Sci.* 10, 27–37. doi:10.1016/j.als.2016.04.001

Aranaz, I., Alcántara, A. R., Civera, M. C., Arias, C., Elorza, B., Heras Caballero, A., et al. (2021). Chitosan: An overview of its properties and applications. *Polymers* 13, 3256. doi:10.3390/polym13193256

ASTM D1708-18 (2018). *Standard test method for tensile properties of plastics by use of microtensile specimens*. West Conshohocken, PA: ASTM International. doi:10.1520/D1708-18

ASTM D882-18 (2018). *Test method for tensile properties of thin plastic sheeting*. West Conshohocken, PA: ASTM International. doi:10.1520/D0882-18

Baji, A., Mai, Y.-W., Wong, S.-C., Abtahi, M., and Chen, P. (2010). Electrospinning of polymer nanofibers: Effects on oriented morphology, structures and tensile properties. *Compos. Sci. Technol.* 70, 703–718. doi:10.1016/j.compscitech.2010.01.010

Baker, S. R., Banerjee, S., Bonin, K., and Guthold, M. (2016). Determining the mechanical properties of electrospun poly-ε-caprolactone (PCL) nanofibers using AFM and a novel fiber anchoring technique. *Mater. Sci. Eng. C* 59, 203–212. doi:10.1016/j.msec.2015.09.102

Bose, S., Vu, A. A., Emshadi, K., and Bandyopadhyay, A. (2018). Effects of polycaprolactone on alendronate drug release from Mg-doped hydroxyapatite coating on titanium. *Mater. Sci. Eng. C* 88, 166–171. doi:10.1016/j.msec.2018.02.019

Chou, S.-F., Carson, D., and Woodrow, K. A. (2015). Current strategies for sustaining drug release from electrospun nanofibers. *J. Control. Release* 220, 584–591. doi:10.1016/j.jconrel.2015.09.008

Chou, S.-F., and Woodrow, K. A. (2017). Relationships between mechanical properties and drug release from electrospun fibers of PCL and PLGA blends. *J. Mech. Behav. Biomed. Mater.* 65, 724–733. doi:10.1016/j.jmbbm.2016.09.004

Cooper, A., Floreani, R., Ma, H., Bryers, J. D., and Zhang, M. (2013). Chitosan-based nanofibrous membranes for antibacterial filter applications. *Carbohydr. Polym.* 92, 254–259. doi:10.1016/j.carbpol.2012.08.114

Croisier, F., Duwez, A.-S., Jérôme, C., Léonard, A. F., van der Werf, K. O., Dijkstra, P. J., et al. (2012). Mechanical testing of electrospun PCL fibers. *Acta Biomater.* 8, 218–224. doi:10.1016/j.actbio.2011.08.015

Cui, W., Cheng, L., Li, H., Zhou, Y., Zhang, Y., and Chang, J. (2012). Preparation of hydrophilic poly(L-lactide) electrospun fibrous scaffolds modified with chitosan for enhanced cell biocompatibility. *Polymer* 53, 2298–2305. doi:10.1016/j.polymer.2012.03.039

Dai, T., Tanaka, M., Huang, Y.-Y., and Hamblin, M. R. (2011). Chitosan preparations for wounds and burns: Antimicrobial and wound-healing effects. *Expert Rev. Anti-infective Ther.* 9, 857–879. doi:10.1586/eri.11.59

de Cassan, D., Sydow, S., Schmidt, N., Behrens, P., Roger, Y., Hoffmann, A., et al. (2018). Attachment of nanoparticulate drug-release systems on poly(ε-caprolactone) nanofibers via a graftpolymer as interlayer. *Colloids Surfaces B Biointerfaces* 163, 309–320. doi:10.1016/j.colsurfb.2017.12.050

Emerine, R., and Chou, S.-F. (2022). Fast delivery of melatonin from electrospun blend polyvinyl alcohol and polyethylene oxide (PVA/PEO) fibers. *AIMSBOA* 9, 178–196. doi:10.3934/bioeng.2022013

Ferreira, J. L., Gomes, S., Henriques, C., Borges, J. P., and Silva, J. C. (2014). Electrospinning polycaprolactone dissolved in glacial acetic acid: Fiber production, nonwoven characterization, and *in Vitro* evaluation. *J. Appl. Polym. Sci.* 131, 41068. doi:10.1002/app.41068

Gizaw, M., Thompson, J., Faglie, A., Lee, S.-Y., Neuenschwander, P., and Chou, S.-F. (2018). Electrospun fibers as a dressing material for drug and biological agent delivery in wound healing applications. *Bioengineering* 5, 9. doi:10.3390/bioengineering5010009

Hawkins, B. C., Burnett, E., and Chou, S.-F. (2022). Physicomechanical properties and *in vitro* release behaviors of electrospun ibuprofen-loaded blend PEO/EC fibers. *Mater. Today Commun.* 30, 103205. doi:10.1016/j.mtcomm.2022.103205

He, W., Ma, Z., Yong, T., Teo, W. E., and Ramakrishna, S. (2005). Fabrication of collagen-coated biodegradable polymer nanofiber mesh and its potential for endothelial cells growth. *Biomaterials* 26, 7606–7615. doi:10.1016/j.biomaterials.2005.05.049

Hendriks, F. M., Brokken, D., Oomens, C. W. J., Bader, D. L., and Baaijens, F. P. T. (2006). The relative contributions of different skin layers to the mechanical behavior of human skin *in vivo* using suction experiments. *Med. Eng. Phys.* 28, 259–266. doi:10.1016/j.medengphy.2005.07.001

Kanungo, I., Fathima, N. N., Rao, J. R., and Nair, B. U. (2013). Influence of PCL on the material properties of collagen based biocomposites and *in vitro* evaluation of drug release. *Mater. Sci. Eng. C* 33, 4651–4659. doi:10.1016/j.msec.2013.07.020

Kim, M. S., Park, S. J., Gu, B. K., and Kim, C.-H. (2012). Polycaprolactone-chitin nanofibrous mats as potential scaffolds for tissue engineering. *J. Nanomater.* 2012, 1–9. doi:10.1155/2012/635212

Li, W., Shi, L., Zhang, X., Liu, K., Ullah, I., and Cheng, P. (2018). Electrospinning of polycaprolactone nanofibers using H_2O as benign additive in polycaprolactone/glacial acetic acid solution. *J. Appl. Polym. Sci.* 135, 45578. doi:10.1002/app.45578

Liverani, L., Lacina, J., Roether, J. A., Boccardi, E., Killian, M. S., Schmuki, P., et al. (2018). Incorporation of bioactive glass nanoparticles in electrospun PCL/chitosan fibers by using benign solvents. *Bioact. Mater.* 3, 55–63. doi:10.1016/j.bioactmat.2017.05.003

Loh, Q. L., and Choong, C. (2013). Three-dimensional scaffolds for tissue engineering applications: Role of porosity and pore size. *Tissue Eng. Part B Rev.* 19, 485–502. doi:10.1089/ten.teb.2012.0437

Maciel, M. M., Ribeiro, S., Ribeiro, C., Francesko, A., Maceiras, A., Vilas, J. L., et al. (2018). Relation between fiber orientation and mechanical properties of nano-engineered poly(vinylidene fluoride) electrospun composite fiber mats. *Compos. Part B Eng.* 139, 146–154. doi:10.1016/j.compositesb.2017.11.065

Pailler-Mattei, C., Bec, S., and Zahouani, H. (2008). *In vivo* measurements of the elastic mechanical properties of human skin by indentation tests. *Med. Eng. Phys.* 30, 599–606. doi:10.1016/j.medengphy.2007.06.011

Park, K. E., Jung, S. Y., Lee, S. J., Min, B.-M., and Park, W. H. (2006). Biomimetic nanofibrous scaffolds: Preparation and characterization of chitin/silk fibroin blend nanofibers. *Int. J. Biol. Macromol.* 38, 165–173. doi:10.1016/j.ijbiomac.2006.03.003

Peña, J., Corrales, T., Izquierdo-Barba, I., Doadrio, A. L., and Vallet-Regí, M. (2006). Long term degradation of poly(ε-caprolactone) films in biologically related fluids. *Polym. Degrad. Stab.* 91, 1424–1432. doi:10.1016/j.polymdegradstab.2005.10.016

Poornima, B., and Korrapati, P. S. (2017). Fabrication of chitosan-polycaprolactone composite nanofibrous scaffold for simultaneous delivery of ferulic acid and resveratrol. *Carbohydr. Polym.* 157, 1741–1749. doi:10.1016/j.carbpol.2016.11.056

Qasim, S., Zafar, M., Najeeb, S., Khurshid, Z., Shah, A., Husain, S., et al. (2018). Electrospinning of chitosan-based solutions for tissue engineering and regenerative medicine. *IJMS* 19, 407. doi:10.3390/ijms19020407

Roozbahani, F., Sultana, N., Fauzi Ismail, A., and Nouparvar, H. (2013). Effects of chitosan alkali pretreatment on the preparation of electrospun PCL/Chitosan blend nanofibrous scaffolds for tissue engineering application. *J. Nanomater.* 2013, 1–6. doi:10.1155/2013/641502

Saghazadeh, S., Rinoldi, C., Schot, M., Kashaf, S. S., Sharifi, F., Jalilian, E., et al. (2018). Drug delivery systems and materials for wound healing applications. *Adv. Drug Deliv. Rev.* 127, 138–166. doi:10.1016/j.addr.2018.04.008

Sapkota, S., and Chou, S.-F. (2020). Electrospun chitosan-based fibers for wound healing applications. *J. Biomaterials* 4, 51–57. doi:10.11648/j.jb.20200402.13

Sarasam, A., and Madihally, S. (2005). Characterization of chitosan–polycaprolactone blends for tissue engineering applications. *Biomaterials* 26, 5500–5508. doi:10.1016/j.biomaterials.2005.01.071

Schneider, A., Wang, X. Y., Kaplan, D. L., Garlick, J. A., and Egles, C. (2009). Biofunctionalized electrospun silk mats as a topical bioactive dressing for accelerated wound healing. *Acta Biomater.* 5, 2570–2578. doi:10.1016/j.actbio.2008.12.013

Surucu, S., and Turkoglu Sasmazel, H. (2016). Development of core-shell coaxially electrospun composite PCL/chitosan scaffolds. *Int. J. Biol. Macromol.* 92, 321–328. doi:10.1016/j.ijbiomac.2016.07.013

Tan, E. P. S., Ng, S. Y., and Lim, C. T. (2005). Tensile testing of a single ultrafine polymeric fiber. *Biomaterials* 26, 1453–1456. doi:10.1016/j.biomaterials.2004.05.021

Tarafder, S., and Bose, S. (2014). Polycaprolactone-coated 3D printed tricalcium phosphate scaffolds for bone tissue engineering: *In vitro* alendronate release behavior and local delivery effect on *in vivo* osteogenesis. *ACS Appl. Mater. Interfaces* 6, 9955–9965. doi:10.1021/am501048n

Tarafder, S., Nansen, K., and Bose, S. (2013). Lovastatin release from polycaprolactone coated β-tricalcium phosphate: Effects of pH, concentration and drug–polymer interactions. *Mater. Sci. Eng. C* 33, 3121–3128. doi:10.1016/j.msec.2013.02.049

Trinca, R. B., Westin, C. B., da Silva, J. A. F., and Moraes, Â. M. (2017). Electrospun multilayer chitosan scaffolds as potential wound dressings for skin lesions. *Eur. Polym. J.* 88, 161–170. doi:10.1016/j.eurpolymj.2017.01.021

Wachirahuttapong, S., Thongpin, C., and Sombatsompop, N. (2016). Effect of PCL and compatibility contents on the morphology, crystallization and mechanical properties of PLA/PCL blends. *Energy Procedia* 89, 198–206. doi:10.1016/j.egypro.2016.05.026

Wang, J., and Windbergs, M. (2017). Functional electrospun fibers for the treatment of human skin wounds. *Eur. J. Pharm. Biopharm.* 119, 283–299. doi:10.1016/j.ejpb.2017.07.001

Wang, S., Li, Y., Zhao, R., Jin, T., Zhang, L., and Li, X. (2017). Chitosan surface modified electrospun poly(ε-caprolactone)/carbon nanotube composite fibers with enhanced mechanical, cell proliferation and antibacterial properties. *Int. J. Biol. Macromol.* 104, 708–715. doi:10.1016/j.ijbiomac.2017.06.044

Wong, S.-C., Baji, A., and Leng, S. (2008). Effect of fiber diameter on tensile properties of electrospun poly(ε-caprolactone). *Polymer* 49, 4713–4722. doi:10.1016/j.polymer.2008.08.022

Xue, W., Bandyopadhyay, A., and Bose, S. (2009). Polycaprolactone coated porous tricalcium phosphate scaffolds for controlled release of protein for tissue engineering. *J. Biomed. Mater. Res.* 91B, 831–838. doi:10.1002/jbm.b.31464

Yang, X., Chen, X., and Wang, H. (2009). Acceleration of osteogenic differentiation of preosteoblastic cells by chitosan containing nanofibrous scaffolds. *Biomacromolecules* 10, 2772–2778. doi:10.1021/bm900623j

Yao, Q., Cosme, J. G. L., Xu, T., Miszuk, J. M., Picciani, P. H. S., Fong, H., et al. (2017). Three dimensional electrospun PCL/PLA blend nanofibrous scaffolds with significantly improved stem cells osteogenic differentiation and cranial bone formation. *Biomaterials* 115, 115–127. doi:10.1016/j.biomaterials.2016.11.018

Yao, Y., Wang, J., Cui, Y., Xu, R., Wang, Z., Zhang, J., et al. (2014). Effect of sustained heparin release from PCL/chitosan hybrid small-diameter vascular grafts on anti-thrombogenic property and endothelialization. *Acta Biomater.* 10, 2739–2749. doi:10.1016/j.actbio.2014.02.042